ISSN NO. 2320-5407

Journal homepage: http://www.journalijar.com

INTERNATIONAL JOURNAL OF ADVANCED RESEARCH

RESEARCH ARTICLE

Turbulent forced convection in a curved duct

Bouaraour Kamel [(1)] and Belaid Abdelfateh [(2)]

1. Department of Sciences and Technology, Ghardaia University. Ghardaia. Algeria
2. Laboratory of Transport Engineering and Environment, Constantine University 1.Constantine. Algeria

Manuscript Info

Manuscript History:

Received: 18 July 2015
Final Accepted: 29 August 2015
Published Online: September 2015

Key words:

Turbulent flow, Forced convection, Curved duct, Numerical simulation.

Corresponding Author

Bouaraour Kamel

Abstract

This study presents the 2D numerical simulation results of turbulent forced flow in a curved duct using Fluent code. Governing equations are discretized using finite volume method with a staggered grid. Reynolds number based on the duct width and the inlet velocity takes several values: Re= 10^4, 6.10^4, $10^5$and 5.10^5. Effect of inlet turbulent intensity is also discussed, by varying it from 1% to 10%. After the validation of the numerical method, results show good agreement as compared to the experimental data. The turbulent flow field characteristics are given by velocity and shear stress in many cross sections inside the duct. We found that increasing Reynolds number modifies the flow structure and we concluded also that the increase of the inlet intensity gives higher values of turbulent quantities for the same Reynolds number.

INTRODUCTION

Fluid motion through curved ducts is a common occurrence in a wide range of industrial applications, such as in gas turbine blades, air conditioning, heat exchangers and nuclear reactors. Dean [1] was the first to investigate the secondary flow in curved ducts, results from the superposition of two forces: the centrifugal force due to the streamwise curvature and the driving pressure gradient. The secondary flow depends on a dimensionless parameter called Dean number.

Many earlier studies focus on the laminar convection in curved ducts, including the effect of different parameters on the flow field and heat transfer like the Dean number (and corresponding Reynolds numbers) [2-3], the aspect ratios and the Prandtl number [4] and the buoyancy effect[5-6].

The duct curvature and the duct cross section have a great influence on the fluid flow and heat transfer which is higher than in straight ducts. Transition to turbulence is delayed in curved ducts due to the stabilizing contribution of the secondary flow generated by centrifugal forces as mentioned by White [7].Few studies have focused on the dependence between Dean instability and curvature ratio, where Dean number is between 25 and 500 [8-10].There is a need for having a good understanding of the fluid flow in curved ducts, and the need to explore the feasibility of obtaining an optimum configuration for high Reynolds numbers. In the present work, incompressible viscous turbulent flow characteristics in a curved duct are investigated numerically. Governing equations are discretized by the finite volume method and resolved by the Fluent code. Results are discussed for different Reynolds numbers greater than $10^4$and for different inlet turbulent intensities between 1% and 10%.

1) Configuration

Turbulent forced convection of air in a curved duct has been considered. The computation domain is formed by a curved duct with an inner and outer radius of R_1 and R_2 respectively. Fig.1 shows the configuration of the considered problem where R denotes the medium radius of curvature and D the width of the duct.

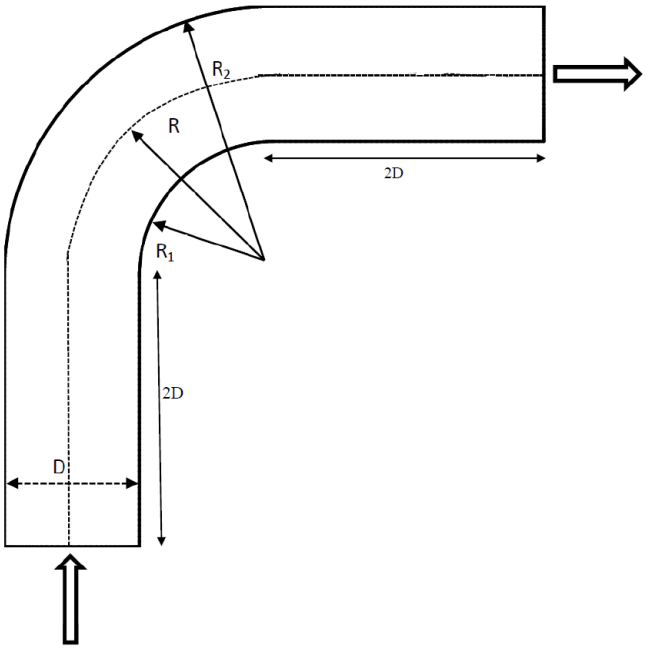

Fig. 1: System Configuration

2) Governing equations and boundary conditions

The governing equations for turbulent forced convection flow is described mathematically by the Reynolds averaged Navier-Stokes equations (RANS). The RANS equations for the velocity field are as follows:

$$\frac{\partial(\rho U_i)}{\partial X_i} = 0 \qquad (1)$$

$$\frac{\partial(\rho U_i)}{\partial t} + \frac{\partial(\rho U_i U_j)}{\partial X_j} = -\frac{\partial P}{\partial X_i} + \frac{\partial}{\partial X_j}\left[\mu\frac{\partial U_i}{\partial X_j} - \rho\overline{u_i u_j}\right] \qquad (2)$$

Where turbulence stress is approximated as:

$$-\rho\overline{u_i u_j} = \mu_t\left(\frac{\partial U_i}{\partial X_j} + \frac{\partial U_j}{\partial X_i}\right) - \frac{2}{3}\rho\delta_{ij}K \qquad (3)$$

Where the Kronecker delta is given by $\delta_{ij}=1$ if (i=j) and $\delta_{ij}=0$ if ($i \neq j$). Turbulence is modeled with the RNG based k- ε model derived from the instantaneous Navier-Stokes equations, using a mathematical technique called renormalization group RNG methods. The RNG model is an eddy-viscosity model similar to the standard k-ε model, but incorporates near wall turbulence anisotropy and non-local pressure-strain effects. It is a general low-Reynolds number turbulence model that is valid all the way up to solid walls, and therefore does not need to make use of wall functions.

$$\frac{\partial(\rho K)}{\partial t} + \frac{\partial(\rho U_i K)}{\partial X_i} = \frac{\partial}{\partial X_i}\left(\mu + \frac{\mu_t}{\sigma_K}\frac{\partial K}{\partial X_i}\right) + P_K - \rho\varepsilon \qquad (4)$$

$$\frac{\partial(\rho\varepsilon)}{\partial t} + \frac{\partial(\rho U_i \varepsilon)}{\partial X_i} = \frac{\partial}{\partial X_i}\left(\mu + \frac{\mu_t}{\sigma_\varepsilon}\frac{\partial \varepsilon}{\partial X_i}\right) + C_{\varepsilon 1}\frac{\varepsilon}{K}P_K - C_{\varepsilon 2}\frac{\rho\varepsilon^2}{K} - R_\varepsilon \qquad (5)$$

The analytical derivation results in a model with constants that are different from those employed in the standard k-ε model, where P_k is the sheer production of turbulence kinetic energy. R_ε is an additional term related to mean strain and turbulence quantities as:

$$R_\varepsilon = \frac{C_\mu\rho\eta^3\left(1-\frac{\eta}{\eta_0}\right)}{1+\beta'\eta^3}\frac{\varepsilon^2}{K} \qquad (6)$$

With:

$$\eta = \sqrt{2S_{ij}S_{ij}}\,\frac{K}{\varepsilon} \qquad (7)$$

And the strain tensor is defined as:

$$S_{ij} = \frac{1}{2}\left(\frac{\partial U_i}{\partial X_j} + \frac{\partial U_j}{\partial X_i}\right) \qquad (8)$$

The constants of this model are presented in table 1.

C□	C□1	C□2	□□	□’
0.0845	1.42	1.68	4.38	0.012

Table 1: Constants of RNG k-ε model

The boundary conditions for the considered problem can be expressed as:

- The velocity at the gap of the inlet is: $V=V_{in}$ and $U_{in}=0$. Turbulent kinetic energy and dissipation at the inlet are respectively: $K_{in}=1.5(V_{in}I_0)^2$ and $\varepsilon_{in}=K_{in}^{1.5}/\ell$. ℓ: is a turbulent length scale (ℓ=D/20) andI_0 is the inlet turbulent intensity.
- At the outlet, gradients of all variables in the x- direction are set to zero.
- The velocity boundary conditions are fixed as zero over the solid walls.

3) Numerical methods

The governing equations are discretized using finite volumes method [11] and the solver is the commercial CFD code FLUENT 6.3. The velocity components are calculated at a staggered grid while the scalar variables are calculated at the main grid (not staggered). For coupling of mass and momentum equations, SIMPLE algorithm with second order upwinding for momentum solution was considered [12]. The discretization of pressure is based on the PRESTO! scheme. The convergence criterion was taken 5.10^{-6} for the residual of each equation. We have used relaxation factors of 0.7 for velocities and 0.3for the pressure. The current numerical CFD code has been applied with success to validate many numerical studies in natural turbulent cases [13-15], forced turbulent case [16] and mixed turbulent cases [17-18].

4) Results and discussion

To understand flow field features inside the curved duct, four Reynolds numbers are considered: Re = 10^4, 6.10^4 , 10^5 and 5.10^5 . Prandtl number is fixed to 0.71 and the time step is fixed to 10^{-4}.

5-1) Grid independence and code validation

Numerical results are obtained with non-uniform meshes of different grid sizes: 3600, 4725 and 6000 cells. The mesh is tighter near solid walls to account for boundary layer generation. The structured non-uniform grid distribution is shown in Fig. 2.

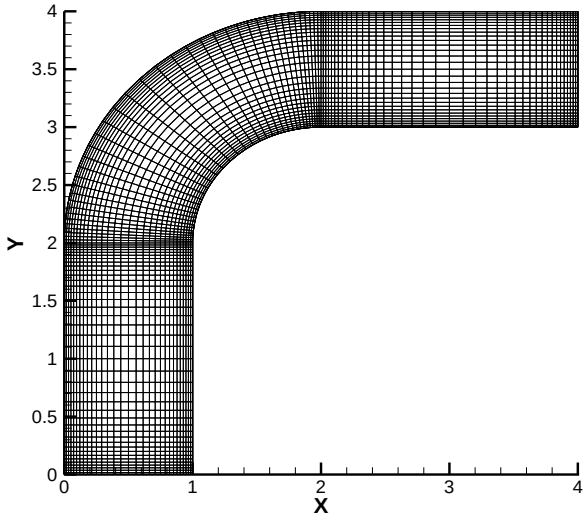

Fig. 2: Mesh and coordinates for the geometrical configuration

For Re = 10^5, the deviation between the two last meshes was less than 0.15% for the maximum vertical velocity and less than 0.28% for the maximum horizontal velocity. Maximum turbulent viscosity deviation reaches 0.075%, so the mesh 3 was adopted.

	Mesh1	Mesh 2	Mesh 3
V_{max} (m/s)	1.520	1.531	1.529
U_{max} (m/s)	1.456	1.466	1.470
$\square_{tmax}$ (m^2/s)	0.002728	0.002738	0.002736

Table 2: Deviation between meshes

To validate the mathematical model and numerical methods, it has been tested with the experimental results of the natural turbulent convection in a square cavity available in the literature [15], where vertical walls are maintained at uniform and different temperatures, while the horizontal walls are kept insulated. The cavity height is 0.75 m and its width is 0.75 m and the temperature difference was 40 K, which gives a Rayleigh number of: $1.58x10^9$. The number of iterations needed to converge was more than 10^6. Fig. 3 shows numerical results of the mean temperature at mid-height compared to the experimental data.

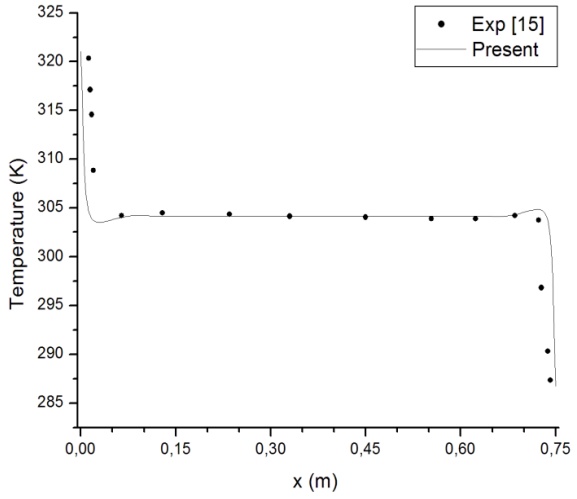

Fig.3: Comparison of predicted temperature profile at mid-height of the square cavity with experimental data [15].

5-2)Flow field inside the curved duct

Reynolds number based on the inlet width and the inlet air velocity takes different values: $Re=10^4$, 6.10^4,$10^5$and 5.10^5. Interaction between airflow and pressure gradient imply the presence of primary and secondary recirculation. The compute vertical velocity contours inside the curved duct are shown in Fig.4.

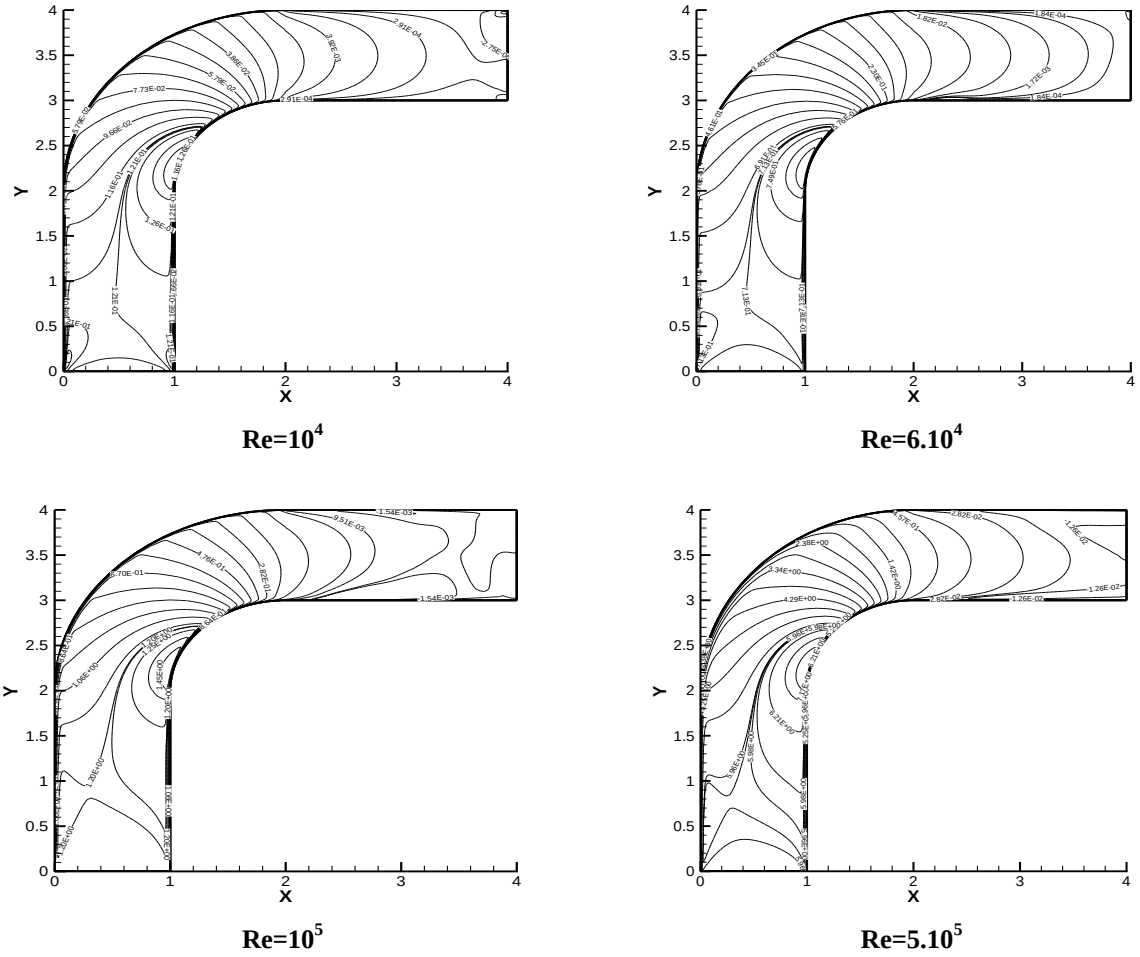

Fig. 4: Contours plot of mean vertical velocity

For $Re=10^4$,maximum value is near the center of curvature. The fluid particles close to the center have larger centrifugal forces than the others near the inlet, and they tend to push the fluid far away from the center of curvature. Increasing Reynolds number, the velocity contours are fairly the same and the variation are not very significant.

Mean vertical velocity profiles are shown in Fig. 5. For three arbitrary vertical positions, we can conclude that their behaviors are qualitatively the same when increasing Reynolds numbers. However, maximum values are always proportional to the Reynolds number. We have concluded that for Y=D/2 and Y=D, the vertical velocity profiles are almost symmetric for X=0.5 (for the same Reynolds number), however for Y=2D this symmetry is broken. We have concluded also that convergence is faster for the higher Reynolds numbers.

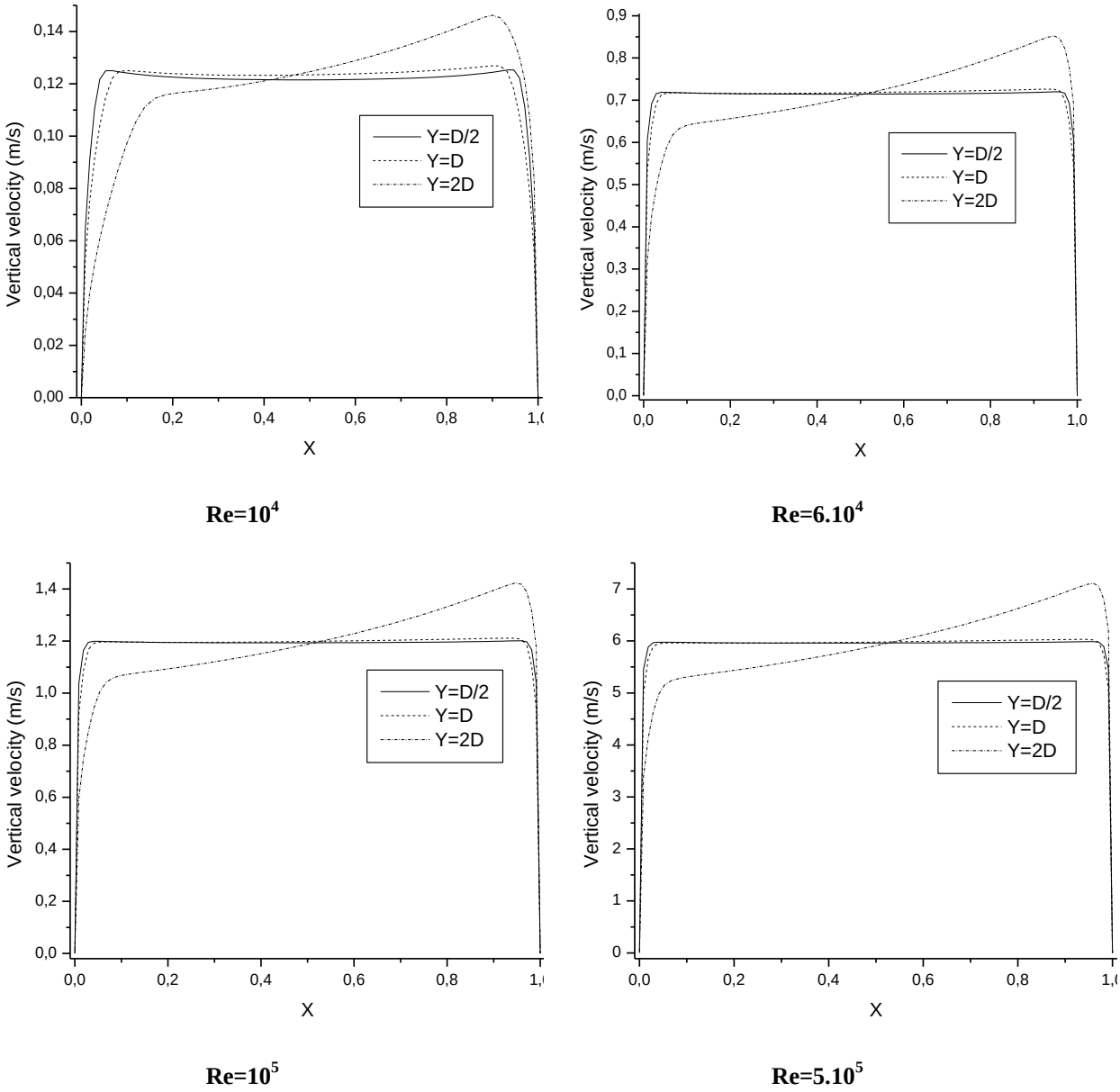

Fig. 5: Mean vertical velocity profiles

5-3) Shear stresses and friction factor

The friction factor is one of the most important parameters which must be taken into account. The friction coefficient is related to the shear stress by the relation:

$$C_f = \frac{1}{2}\frac{\tau_w}{\rho V_{in}^{\ 2}} \qquad (9)$$

The numerical results for the friction factor for the inner and the outer wall are shown in Fig 6.

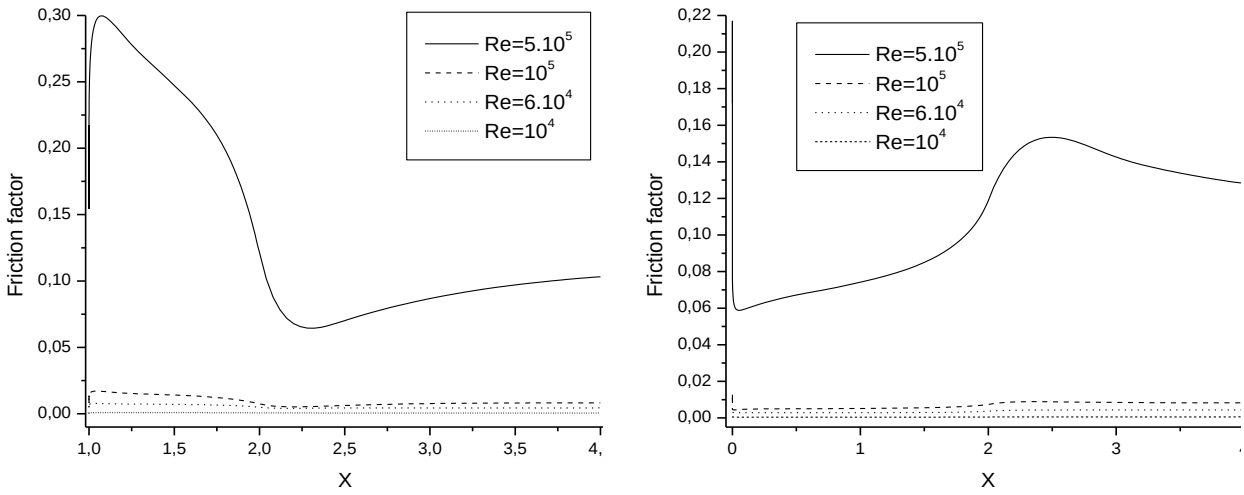

(a) (b)

Fig. 6: Friction factor for inner wall (a) and outer wall (b)

For the inner and the outer wall, the friction factor remains almost constant for Reynolds numbers between 10^4 and 10^5. There is only one peak located near the wall for Re=5.10^5 for the inner wall. The friction coefficient decreases until reaches the minimum at X=2.25 which corresponding to the curved surface of the inner wall. Then it increases almost linearly for the rest portion of the duct. However, for the outer duct, behaviors are different due to the centrifugal force acting to the curved portion of the outer wall, where friction coefficient reaches its maximum.

5-4) Effect of inlet turbulent intensity

To understand the effect of inlet turbulent intensity on the flow characteristics and turbulent quantities, we have considered three inlet turbulent intensities: I_0=1%, I_0=5% and I_0=10%. Fig.7 shows the evolution of the turbulent kinetic energy for Y=2D. The evolution is qualitatively similar for Re= $10^4$and for Re=6.10^4 for the three chosen inlet intensities. Turbulent kinetic energy decreases almost linearly near the outer wall. The decrease immediately after the inlet is caused by the increase of the centerline velocity due to boundary layer growth. An insignificant variation between the walls of the duct is observed, and then a sudden decrease near the inner wall of the duct is detected. However, the evolution for Re= 10^5 and for Re=5.10^5 is quite different especially for the high intensities. The common feature for all Reynolds numbers considered, is that the maximum values are always depending on the inlet intensity.

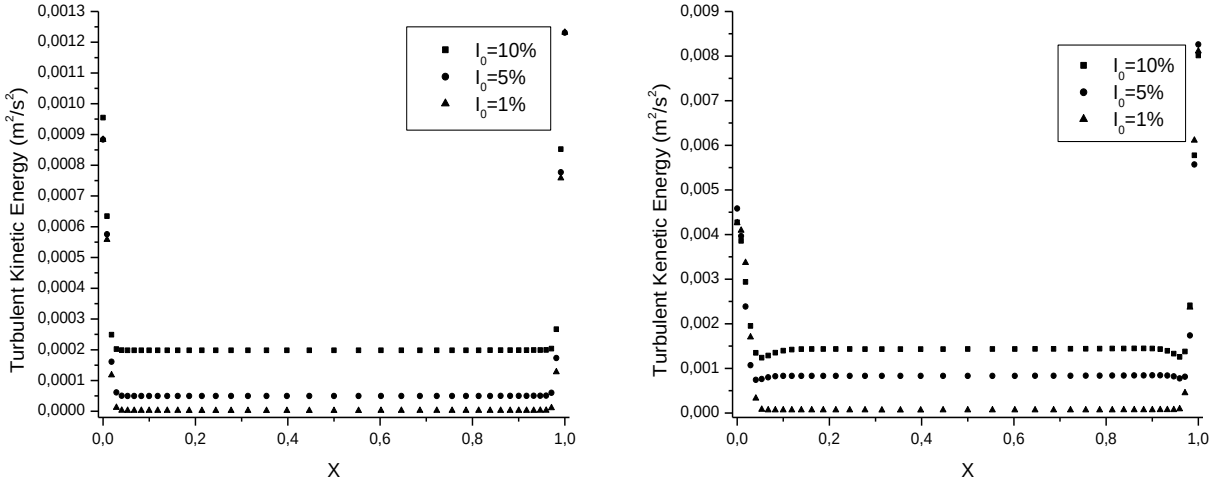

Re=10^4 **Re=6.10^4**

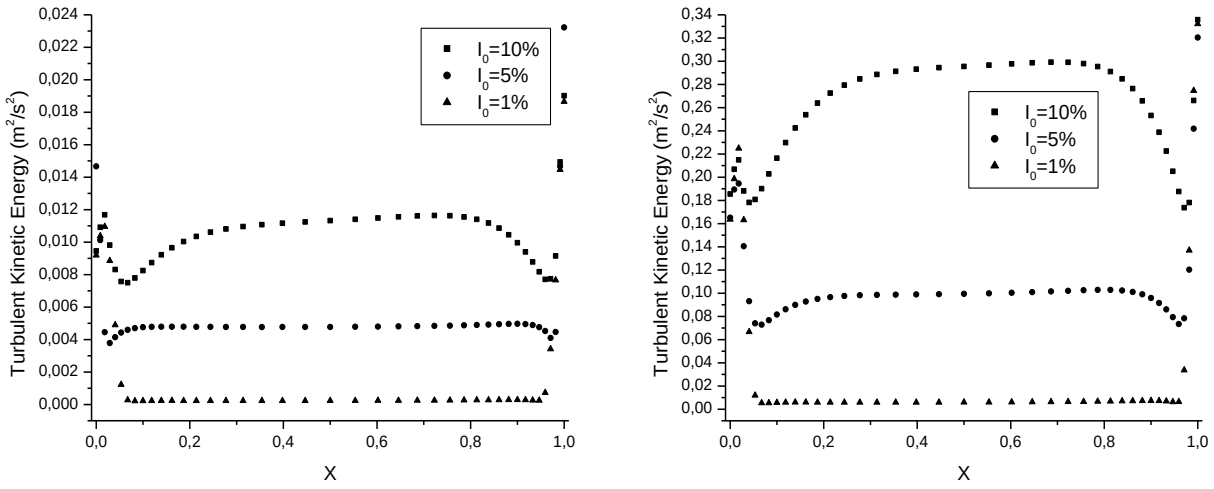

Re=10^5 **Re=5.10^5**

Fig. 7: Turbulent kinetic energy for Y=2D

Conclusion

In this paper a numerical simulation of turbulent forced convection inside a curved duct was presented. Results are discussed for different Reynolds numbers and for different turbulent intensities at the duct inlet. After the validation of the mathematical model and numerical methods, it was found that the variation of the Reynolds number from Re=$10^4$to 5.10^5affects the airflow patterns, velocity and turbulent characteristics inside the curved duct. The following remarks can be made:

- For the same Reynolds number, turbulent kinetic energy profiles are qualitatively the same for the different inlet intensities. However, maximum values are always for the higher intensities.
- The considered Reynolds numbers make the flow inside the cavity dominated by inertia forces and the centrifugal force is proportional to the inlet velocity.
- Vertical velocity profiles in many vertical positions have qualitatively the same behavior for the considered Reynolds numbers.
- Maximum values of the friction coefficient are encountered near the curved surface of the outer wall due to the centrifugal force, and near the inner wall in the straight portion of the duct at the inlet.

Nomenclature

D: Width of the duct (m)
Cp: Specific heat at constant pressure (J/Kg.K)
U, V: Velocity components along x and y directions (m/s)
P: Pressure (Pa)
t: Time (s)
K: Turbulent kinetic energy (m^2/s^2)
I_0: Turbulence intensity at the inlet

$\Pr = \frac{\nu}{\alpha}$: Prandtl number

$\mathrm{Re} = \frac{V_{in} D}{\nu}$: Reynolds number

De: Dean number

Greek symbols

ε: Turbulent Dissipation rate (m^2/s^3)
δ_{ij}: Kronecker delta

Subscripts

max: maximum
in: inlet

References

[1] W.R. Dean, Fluid motion in a curved channel, Proc. R. Soc. London, Ser. A 121 (1928) 402–420.
[2] G. J. Hwang and C.-H.Chao, Forced Laminar Convection in a Curved Isothermal Square Duct, Trans. ASME, J. Heat Transfer, vol. 113, pp. 48–55, 1991.
[3] P. M. Ligrani, S. Choi, A. R. Schallert, and P. Skogerboe, Effects of Dean Vortex Pairs on Surface Heat Transfer in Curved Channel Flow, Int. J. Heat Mass Transfer, vol. 39, no. 1, pp. 27–37, 1996.
[4] K. C. Cheng and M. Akiyama, Laminar Forced Convection Heat Transfer in Curved Rectangular Channels, Int. J. Heat Mass Transfer, vol. 13, pp. 471–490, 1970.
[5] R. Chilukuri and J. A. C. Humphrey, Numerical Computations of Buoyancy-Induced Recirculation in Curved Square Duct Laminar Flow, Int. J. Heat Mass Transfer, vol. 24, pp. 305–314, 1981.
[6]T. T. Chandratilleke and Nursubyakto, Numerical Prediction of Secondary Flow and Convective Heat Transfer in Externally Heated Curved Rectangular Ducts, Int. J. Thermal Sci., vol. 42, pp. 187–198, 2003.
[7]C.M. White, Streamline flow through curved pipes, Proceedings of the RoyalSociety A 123 (1929) 645-663.
[8] T.T. Chandratilleke, Secondary Flow Characteristics and Convective HeatTransfer in a Curved Rectangular Duct with External Heating, 5th WorldConference On Experimental Heat Transfer, Fluid mechanics and Thermodynamics,Thessaloniki, Greece, September 2001.
[9] T.T. Chandratilleke, Performance Enhancement of a Heat Exchanger UsingSecondary Flow Effects, in: Proc. of 2nd Pacific-Asia Conf.Mech. Eng., Manila,Philippines, September 1998.
[10] T.T. Chandratilleke, Nursubyakto, Numerical prediction of secondary flow andconvective heat transfer in externally heated curved rectangular ducts,International Journal of Thermal Sciences 42 (2002) 187-198.
[11] H. K. Versteeg and W. Malalasekera, An Introduction to Computational Fluid Dynamics: The Finite Volume Method, Prentice Hall, 1995.
[12] S. V. Patankar, Numerical heat transfer and fluid flow, Mac Graw Hill, New York, 1980.
[13] R. Harish and K. Venkatasubbaiah, Numerical simulation of turbulent plume spread in ceiling vented enclosure, European Journal of Mechanics B/Fluids 42, 142-158, 2013.
[14] S. Wanga, Z. Shena and L. Gub, Numerical simulation of buoyancy-driven turbulent ventilation in attic space under winter conditions, Energy and Buildings 47, 360-368, 2012.
[15] Y. S. Tian and T. G. Karayiannis, Low turbulence natural convection in an air filled square cavity: Part I: The thermal and fluid flow fields, International Journal of Heat and Mass Transfer 43, 849-866, 2000.
[16] S. M. Saeidi and J. M. Khodadadi, Forced convection in a square cavity with inlet and outlet ports, International Journal of Heat and Mass Transfer 49, 1896-1906, 2006.
[17] T. V. Radhakrishnan, A. K. Verma, C. Balaji and S. P. Venkateshan, An experimental and numerical investigation of mixed convection from a heat generating element in a ventilated cavity, Experimental Thermal and Fluid Science 32, 502-520, 2007.
[18] J. Moureh, M. Tapsoba and D. Flick, Airflow in a slot-ventilated enclosure partially filledwith porous boxes: Part II- Measurements and simulations within porous boxes, computersand fluids 38, 206-220, 2009.